



## DETERMINATION OF SPIN-BASED HALF-METALLIC, MECHANICAL, MAGNETIC AND THERMODYNAMIC PROPERTIES OF QUATERNARY HALF-HEUSLERS ZRCOFEX (X=SI, AS AND GE) USING FIRST-PRINCIPLE CALCULATIONS.

<sup>1</sup>Ogundola Sunday and <sup>2</sup>Tantasso Sabo

<sup>1</sup>Department. of Physics, University of Benin, Benin City, Edo state, Nigeria

<sup>2</sup>Department of Physics Electronics, Federal Polytechnic, Mubi, Adamawa state, Nigeria.

### ARTICLE INFO

#### Article history:

Received xxxxx

Revised xxxxx

Accepted xxxxx

Available online xxxxx

#### Keywords:

Quaternary

Heuslers,

Density

functional

Theory,

Half-

metallicity,

Band

structures,

Magnetic

moments.

### ABSTRACT

The First Principle Density Functional Theory (DFT) method was used to investigate the half-metallic character, magnetic and thermodynamic properties of ZrCoFeX (X=Si,As and Ge). Electronic and magnetic properties such as Band structures, Densities of states, and magnetic moments, spin – polarization indices of each alloy are also determined to confirm half-metallicity and ferromagnetism. Thermodynamic properties are also computed using Quantum Espresso-based Thermo\_pw code. The half-metallic band gaps of ZrCoFeAs, ZrCoFeSi and ZrCoFeGe are 0.206eV, 0.205eV and 0.203eV respectively. The spin-up channels in the electronic band structures of ZrCoFeX(X=Si,As and Ge) have indirect energy band gap, indicating that they exhibit half-metallic character. The quaternary Heuslers are accurately ferromagnetic as they all obey Slater Paulin's rule having magnetic moments of 4.0215 $\mu$ B, 4.1573 $\mu$ B and 4.6711 $\mu$ B respectively and are 100% spin-polarized. The Curie Temperatures  $T_c$  of ZrCoFeX(X=Si,As and Ge) are 526K, 859K and 963K respectively. However, only ZrCoFeAs, and ZrCoFeGe preserved their mechanical stability after undergoing stress-strain test. This makes them preferable candidates in the field of semiconductor physics. The heat capacities of ZrCoFeX(X=Si,As and Ge) obey Dulong-petit law showing that they have good thermal applications in optoelectronic devices e.g. Photo diodes, Solar cells etc.

### 1. INTRODUCTION

Heusler compounds or alloys are magnetic intermetallics with face-centered cubic crystal structure and a composition of XYZ, where X and Y are transition metals and Z is in the p-block. There are five types of Heusler alloys or compounds, viz; XYZ is half-Heusler, X<sub>2</sub>YZ is full-Heusler, XX<sup>1</sup>YZ is quaternary Heusler, X<sub>2</sub>Z is binary half-Heusler and X<sub>3</sub>Z is binary full-Heusler. A Heusler can be semiconductor, metal or half-metal, but it is not an insulator. Every Heusler has spin-up and spin-down channels in its electronic band structure. If both spin-up and spin-down channels are metals, the half-Heusler is a metal.

\*Corresponding author: OGUNDOLA SUNDAY

E-mail address: [ogundolasunday01@gmail.com](mailto:ogundolasunday01@gmail.com)

<https://doi.org/10.60787/tnamp.v24.669>

1115-1307 © 2026 TNAMP. ALL RIGHTS RESERVED

If one spin is semiconductor and the other is a metal, then it is half-metallic or a half-metal [4]. Lastly, if both spins are semiconductors then the heusler is a semiconductor. Many of these compounds exhibit properties relevant to spintronics such as magnetoresistance, variations of the Hall effect, ferro, antiferro, and ferro-magnetism, half-metallicity, semi-conductivity with spin filter ability, superconductivity, and topological band structure. Their magnetism results from a double-exchange mechanism between neighbouring magnetic ions in the first Heusler compound discovered. Heuslers derived its name after a German Engineer and Chemist Friedrich Heusler, who studied such a compound,  $\text{Cu}_2\text{MnAl}$  in 1903 which contained copper, manganese and Aluminum.

Heuslers are isoelectronic compounds that are promising thermoelectric materials because of their high power factor and thermal stability. The magnetic materials particularly of the crystallographic phase  $\text{C}_{1b}$  of the half-Heusler compounds have been an active field of research, as a consequence of their frequently emerging novel properties and field of application since their first discovery by Friedrich Heusler in 1903 with the composition of  $\text{Cu}_2\text{MnAl}$  which behaves like a ferromagnet [6]. In 1983, De Groot *et al* discovered half-metallic ferromagnetism in half-Heusler and further revealed their potentials for promising technological applications [14]. Also, the importance of these materials has been uncovered by viewing the novel features of the electronic band structure and magnetic behaviour of quaternary Heuslers  $\text{ZrCoFeX}$  ( $\text{X}=\text{Si}, \text{As}$  and  $\text{Ge}$ ). Over 400 of the Heusler alloys are predicted to be useful as topological insulators and thermoelectric materials [9]. In the same vein, over 350 heuslers are recognized to have good applications in optoelectronics, magnetic tunnel junctions, giant magneto-resistant devices, piezoelectric semiconductors etc. Extensive investigation is carried out on the possibility of half-metallicity and ferromagnetism of the quaternary heuslers  $\text{ZrCoFeX}$  ( $\text{X}=\text{Si}, \text{As}$  and  $\text{Ge}$ ) using Density functional theory approach [10].

The target of recent research related to Heusler materials is to investigate ferromagnetic quaternary heusler compounds exhibiting the magnetic field induced super-elasticity, and large strain-induced changes in the magnetization [4]. Over 400 of the Heusler alloys are predicted to be useful as topological insulators and thermometric materials [7]. Also, over 350 quaternary Heusler alloys are recognized to have good applications in spintronic, optoelectronics, magnetic tunnel functions, giant magneto-resistant devices and piezoelectric semiconductors [15]. Extensive investigation is carried out on the possibility of half-metallicity and ferromagnetism of the quaternary Heuslers  $\text{ZrCoFeX}$  ( $\text{X}=\text{Si}, \text{As}$  and  $\text{Ge}$ ) using first principles calculations. Section 2 of this work comprises the computational methods of determining all the properties under studies, such as structural, mechanical, magnetic and thermodynamic properties of  $\text{ZrCoFeX}$  ( $\text{X}=\text{Si}, \text{As}$  and  $\text{Ge}$ ) Section 3 contains the results and discussions of all the properties calculated in section 2 , while the whole work is summarized under conclusion.

## **2. COMPUTATIONAL DETAILS**

Using quantum espresso that implements Density Functional Theory (DFT), properties of quaternary Heuslers  $\text{ZrCoFeX}$  ( $\text{X}=\text{Si}, \text{As}$  and  $\text{Ge}$ ) are calculated. Extension of electron wave function is done by the plane wave basis set [13]. The Perdew-Burke-Ernzerhot (PBE) type of generalized gradient approximation (GGA) of the exchange correlation functional is selected for accuracy of eigen energy obtained. The ultra-soft version of pseudopotential is selected. Variable cell relaxation is carried out together with the geometric optimization to compute the structural properties of  $\text{ZrCoFeX}$  ( $\text{X}=\text{Si}, \text{As}$  and  $\text{Ge}$ ). Plane wave basis set of kinetic energy cut-off of 1256eV and 1082eV are used, and Monkhorst pack mesh of  $10 \times 10 \times 10$ ,  $9 \times 9 \times 9$  and  $8 \times 8 \times 8$  in the brilloun zone of  $\text{ZrCoFeX}$  ( $\text{X}=\text{Si}, \text{As}$  and  $\text{Ge}$ ) are respectively used [16]. The magnetic moments, spin-polarized band structures and their densities of states (dos) are also computed. The mechanical and

thermodynamic properties of ZrCoFeX(X=Si,As and Ge) are calculated using quantum espresso –based thermo\_pw code.

## RESULTS AND DISCUSSIONS

### 3.1 Total energy and Structural properties

Total energy as a function of lattice constants for the ferromagnetic (FM) and non-magnetic (NM) of ZrCoFeX(X=Si, As and Ge) is computed as shown in Fig. 3.1. It is observed that the ferromagnetic status of ZrCoFeGe is optimized at lowest energy, followed by the ferromagnetic status of ZrCoFeAs and ZrCoFeSi which are almost optimized at the same energy. This indicates that ZrCoFeGe is more ferromagnetic than the others [6]. This is as a result of germanium being a semiconductor while arsenic and silicon are non-metals, although the presence of Zr, Co and Fe as ferromagnetic elements contribute immensely to the ferromagnetic character of the quaternary heusler alloys. Total energy as a function lattice constants (Å) in the ferromagnetic states is fitted to the Birch-Murnaghan equation of state so as to compute the equilibrium lattice constants, bulk moduli and pressure derivatives. All these are presented in Table 1 [8].

Table 1 Lattice constants, Bulk moduli, Pressure derivative, Formation and Cohesive energy of ZrCoFeX(X=Si, As and Ge) in comparison with the work of Bahnes in the Journal of Alloys and Compounds (2017) (\*\*\*).

Alloy	Lattice Constants(Å)	Bulk modulus(Gpa)	Pressure Derivative (B')	Formation Energy $E_f$ ( $R_y$ )	Cohesive Energy ( $E_{Coh}$ ) ( $R_y$ )
ZrCoFeSi	6.21	242	6.22	-1.6864	1.6864
ZrCoFeAs	6.31	248	6.23	-1.7391	1.7391
ZrCoFeGe	6.54	251	6.71	-1.8439	1.8439
CoFeCrP ***	6.59 ***	248***	6.67 ***	-1.8543 ***	1.8543 ***
CoFeCrAs ***	6.74 ***	249***	6.54 ***	-1.7534 ***	1.7534 ***
CoFeCrSb ***	6.94 ***	255***	6.52 ***	-1.7922 ***	1.7922 ***

The quaternary heuslers (XX'YZ) has a crystallographic structure of  $L_2$  type under space  $Fm\bar{3}m$  (No. 225) , and its structure contains four sub-lattices in which the X atoms are placed at the  $4c(\frac{1}{4}, \frac{1}{4}, \frac{1}{4})a_0$  , and  $4d(\frac{3}{4}, \frac{3}{4}, \frac{3}{4})a_0$  , and the Y and Z atoms are localized at the  $4b(\frac{1}{2}, \frac{1}{2}, \frac{1}{2})a_0$  , and  $4a(0,0,0)a_0$  , where  $a_0$  is the lattice parameter of cell [2] . The calculated lattice constants , Bulk moduli and pressure derivatives of ZrCoFeSi , ZrCoFeAs and ZrCoFeGe are shown in Table 1 as (6.21, 6.31, 6.54) Å, (242,248,251)Gpa and (6.22, 6.23, 6.71)  $B'$  respectively. The energy of formation and cohesive energy of ZrCoFeX(X=Si, As and Ge) are also investigated to ascertain whether the quaternary heuslers are structurally and synthesizable in the laboratory. If the result of the formation energy is negative and that of cohesive energy is positive, the material is structurally stable and can be synthesized experimentally and vice versa. This is done by using equation 1 and 2: E.g

$$E_{formation} = Total\ Energy - (Total\ Energy\ per\ atom\ of\ each\ element) \quad (1)$$

$$E_f = E_{ZrCoFeSi}^{Total} - \{E_{Zr}^{Bulk} + E_{Co}^{Bulk} + E_{Fe}^{Bulk} + E_{Si}^{Bulk}\} \quad (2)$$

$$E_{Coh} = \{(E_{Zr}^{Total} + E_{Co}^{Bulk} + E_{Fe}^{Bulk} + E_{Si}^{Bulk}) - E_{ZrCoFeSi}^{Total}\} \quad (3)$$

Where  $E_f$  and  $E_{Coh}$  represent the total formation and cohesive energies of ZrCoFeSi per formula unit respectively while  $E_{Ni}^{Bulk}$  ,  $E_{Co}^{Bulk}$  ,  $E_{Fe}^{Bulk}$  and  $E_{Si}^{Bulk}$  are the total ground state cohesive and formation energies per atom in the bulk of Zr, Co, Fe and Si as individual element of the alloy respectively [5]. The results of formation energy show negative values while those of cohesive

energy are positive, indicating that the quaternary heuslers ZrCoFeX(X=Si, As and Ge) have structural stability and hence can be synthesized experimentally. In the result, it is keenly observed that the formation of energy of ZrCoFeGe shows more negative values than those of ZrCoFeSi and ZrCoFeAs. The cohesive energy of ZrCoGalso shows more positive value. This therefore affirms that ZrCoFeGe is more structurally stable than its other two counterparts. The results of lattice constants, Bulk moduli, pressure derivatives, energies of formation and cohesive energy of ZrCoFeX(X=Si, As and Ge) show good agreement with the work of A. Bahnes in the journal of Alloys and Compounds (2017) [7]. In the Zinc blende structure geometry at the level of PBE-GGA, the obtained total energies data versus the cell volume of ZrCoFeX(X=Si, As and Ge) are fitted by employing empirical Birch-Murnaghan Equation of states to compute the structural properties:

$$E_{TOT}(V) = E_0(V) + \frac{B_0V}{B'(B'-1)} [B_0 \left(1 - \frac{V_0}{v}\right) + \left(\frac{V_0}{v}\right)^{B'}] \quad (4)$$

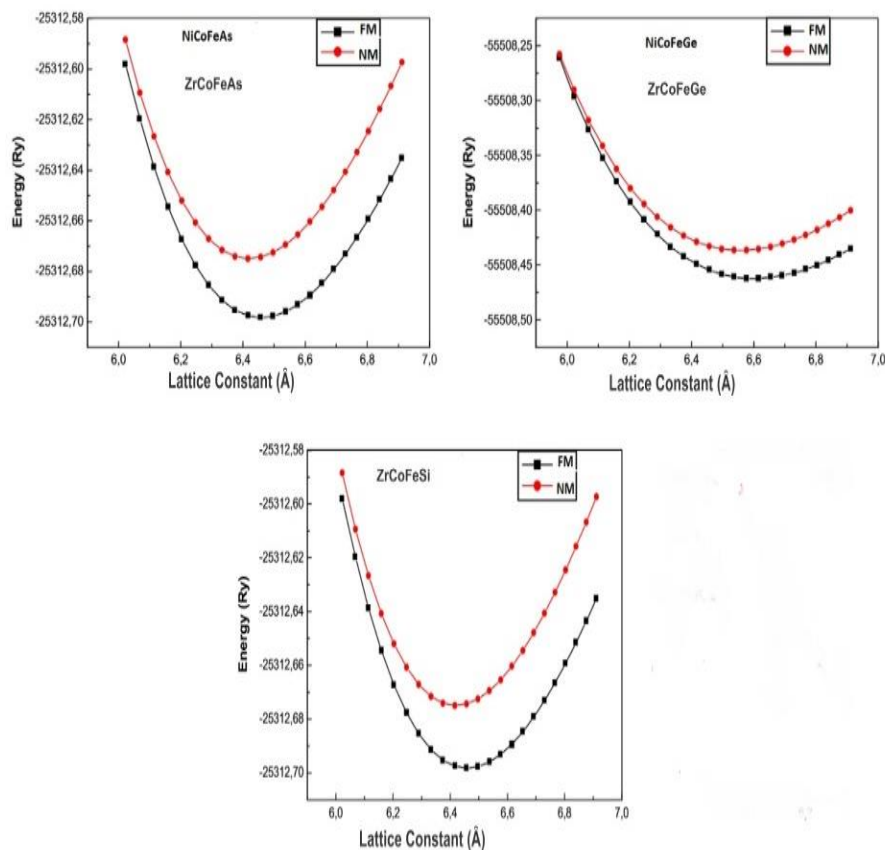


Fig.1.0- Graphs of Energy Vs lattice constants of ZrCoFeX(X=Si, As and Ge) in ferromagnetic and non-magnetic states

### 3.2 Electronic, Half-metallic and Magnetic Properties

The spin-polarized electronic band structures of ZrCoFeX(X=Si, As and Ge) are computed accordingly and shown in fig.2

They are calculated on the basis of structural and PBE-GGA parameters as presented along the high-symmetry direction in the first Brillouin zone (BZ). The majority spin states (spin-up) of the quaternary Heuslers ZrCoFeX(X=Si, As and Ge) exhibit semi-conducting behaviour while the minority spin states (spin-down) of the Heuslers display metallic character [9]. The respective indirect band gaps of ZrCoFeX(X=Si,As and Ge) are 0.205eV, 0.206eV and 0.203eV respectively.

The conduction band minima occur at the G-symmetry points while the valence band maxima occur at L-symmetry points in the band structures of all the alloys with respect to fermi energy level. The computed spin-polarized partial densities of states of ZrCoFeX(X=Si, As and Ge) are also displayed in fig3 [2]. The orbital contributions of valence electrons of each element in the quaternary Heuslers cause the spin-polarization along the fermi energy level. Also, bonding and anti-bonding effects cause band gaps between the conduction band minima and valence band maxima. The valence electrons of Zr, Co, Fe, Si, As and Ge are given as  $(5S^2, 5d^2)$ ,  $(3d^7, 4s^2)$ ,  $(3d^6, 4s^2)$ ,  $(3s^2, 3p^2)$ ,  $(3d^{10}, 4s^2, 4p^3)$  and  $(3d^{10}, 4s^2, 4p^2)$ . D-d orbital interactions within elements enhance spin-polarization of the heuslers along the fermi level [14]. The bonding peaks of Zr, Co, Fe, Si, As and Ge atoms are located in the region below the fermi energy level while the region above the fermi  $E_F$  contains the anti-bonding peaks of the atoms. The contribution of bonding and anti-bonding effect of the atom cause the spin-polarization of the quaternary heuslers. Also, the d-orbital exchange splitting effect of the transition elements Ni, Co and Fe plays vital role in the spin-polarization of the heuslers. This testifies to the half-metallic character ferromagnetic nature and 100% spin-polarization of the quaternary heuslers along the fermi energy level as shown in Table2. The half-metallic energy gap ( $E_{HM}$ ) of Heuslers is expressed as  $HM_{Gap} = \text{Min} (|E_F - E_{VBM}|, |E_F - E_{CBM}|)$ , where  $E_F$ ,  $E_{VBM}$  and  $E_{CBM}$  are the Fermi energy, valence band maximum (VBM) energy and conduction band minimum energy respectively [6].

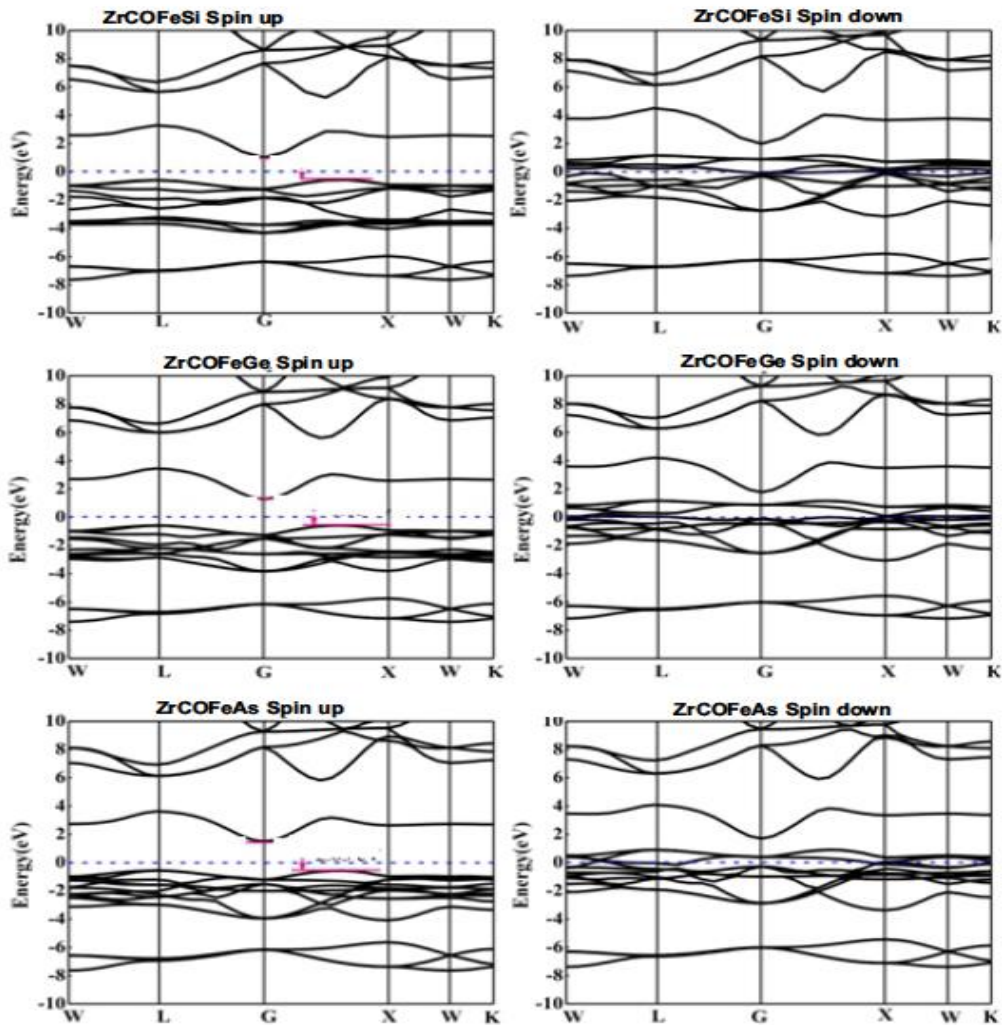
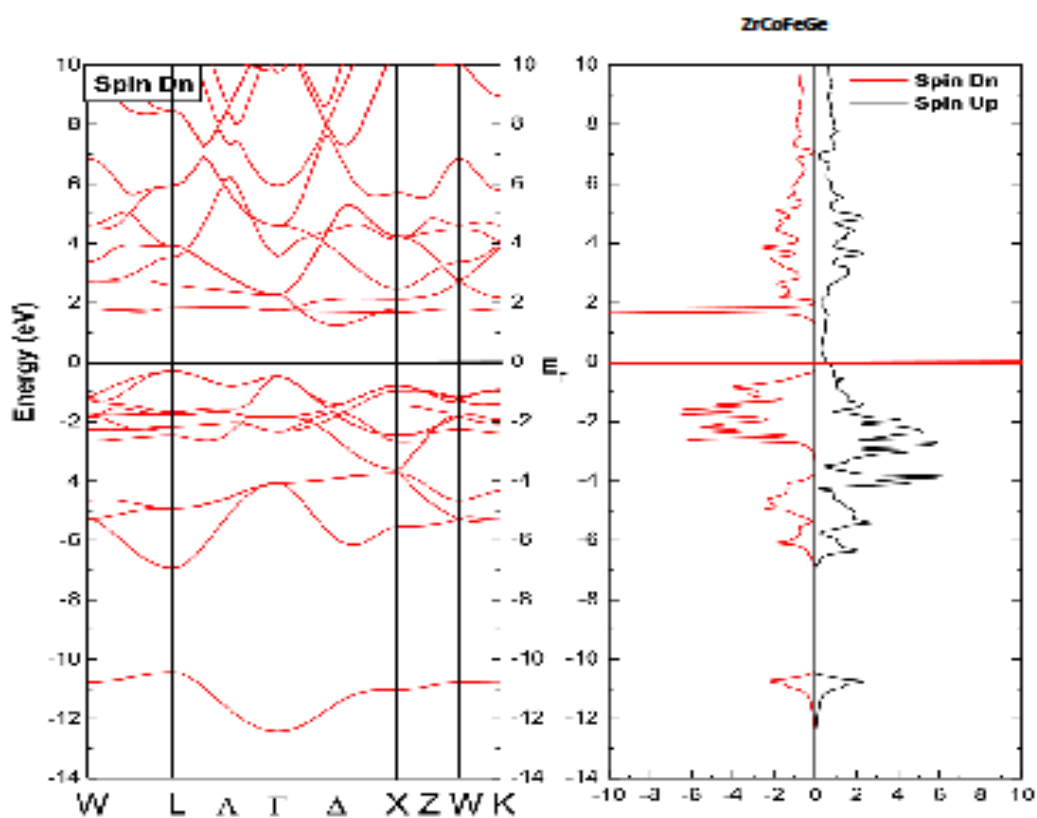
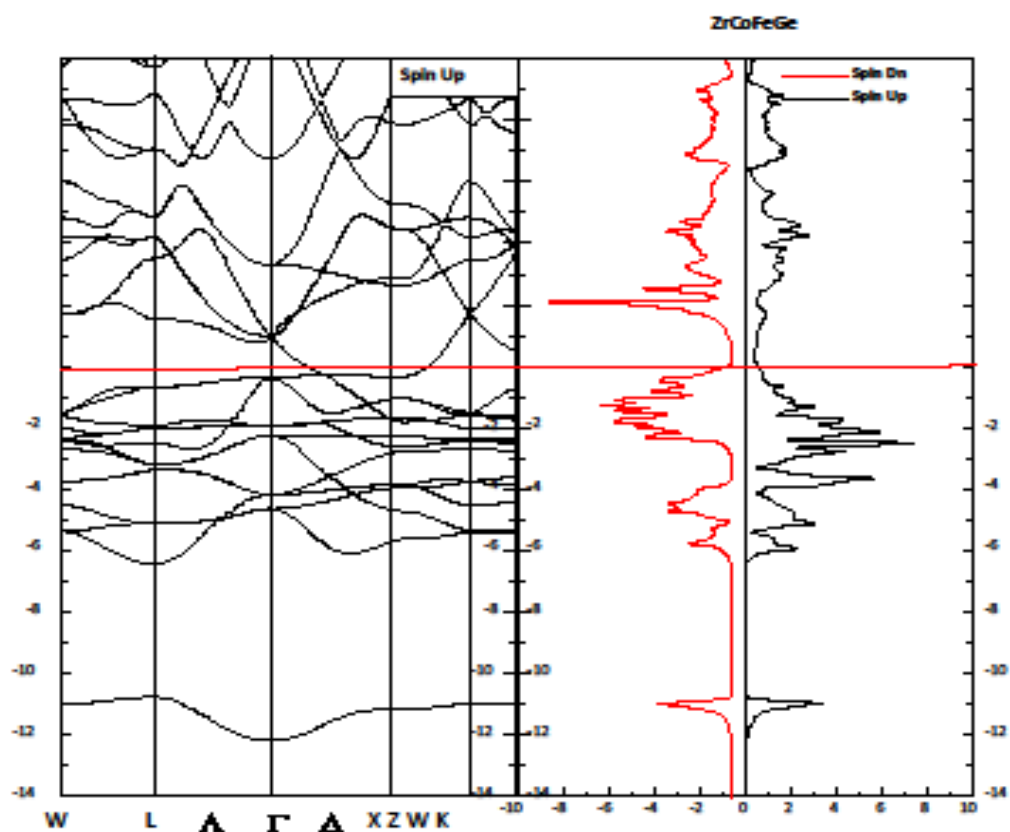


Fig 2 Spin-polarized Electronic Band structures of ZrCoFeSi, ZrCoFeAs and ZrCoFeGe.



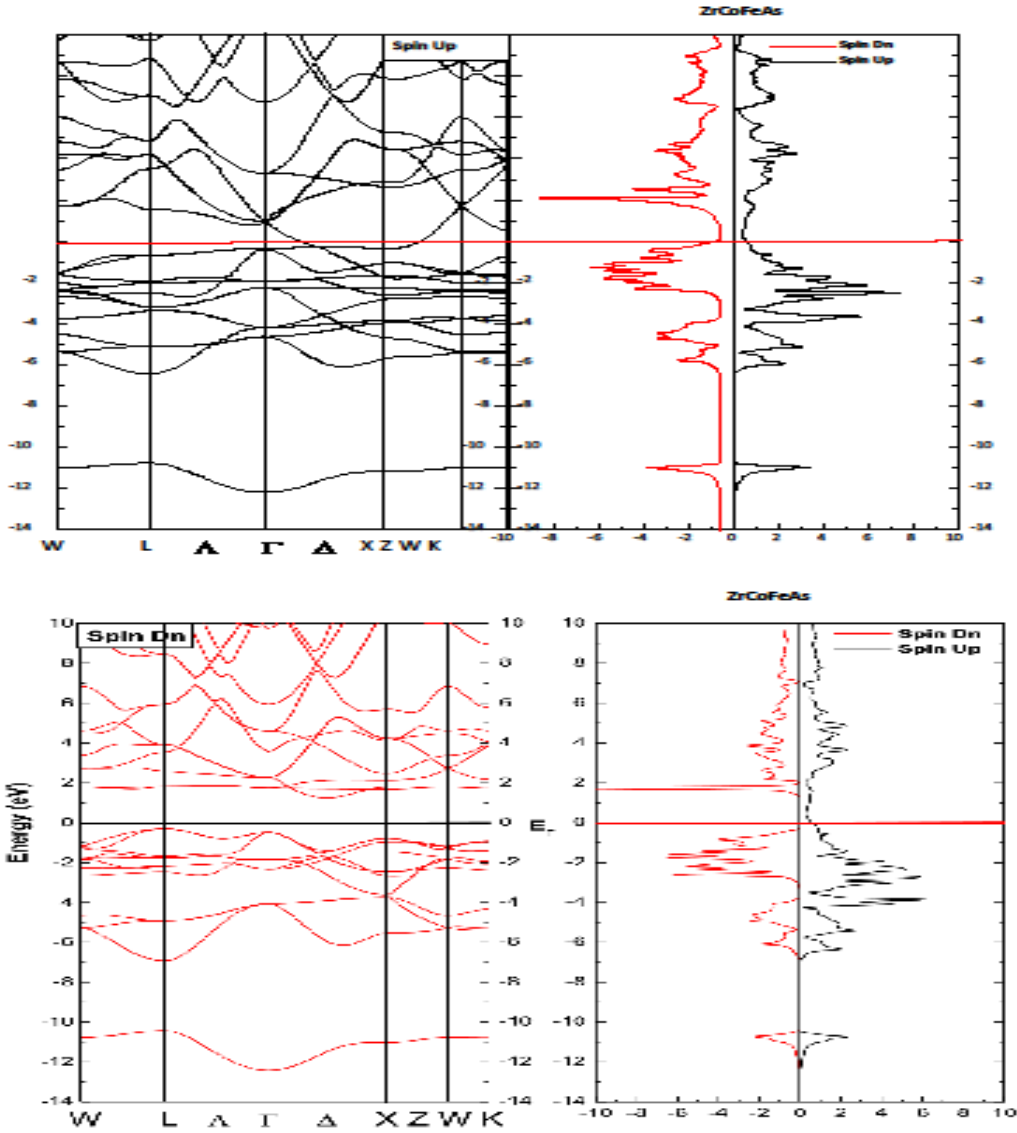


Fig.3 Spin-polarized Partial densities of States of ZrCoFeX(X=Si, As and Ge)

Table 2 Calculated results of the half-metallic gap  $E_{HM}$  (eV), minority spin ( $P \downarrow$ ), majority spin ( $P \uparrow$ ), band gap  $E_g$  (eV) and spin polarization percentage at the Fermi energy level  $E_f$  of ZrCoFeX(X=Si, As and Ge) and CoFeCrZ(Z=P,As and Sb).\*\*\*

Alloy	$E_{HM}(eV)$	$E_g(eV)$	$P \uparrow (eV)$	$P \downarrow (eV)$	$P(\%)$
ZrCoFeSi	0.205	0.205	0.205	0.000	100
ZrCoFeAs	0.206	0.206	0.206	0.000	100
ZrCoFeGe	0.203	0.203	0.203	0.000	100
CoFeCrP ***	1.000 ***	1.000 ***	1.000 ***	0.000 ***	100 ***
CoFeCrAs ***	0.520 ***	0.520 ***	0.520 ***	0.000 ***	100 ***
CoFeCrSb ***	0.750 ***	0.750 ***	0.750 ***	0.000 ***	100 ***

The spin-polarization percentage of a half-metallic material is described by the repartition of the densities of states (DOSs) in spin-up and spin-down cases at the  $E_F$ , which it is defined by the following expression

$$P(\%) = \frac{P\uparrow(E_F) - P\downarrow(E_F)}{P\uparrow(E_F) + P\downarrow(E_F)} \times 100\% \quad (5)$$

Here,  $P\uparrow(E_F)$  and  $P\downarrow(E_F)$  are the densities of majority and minority spin electrons at  $E_F$ , respectively. The complete half-metallic character is observed when  $P\downarrow(E_F)$  or  $P\uparrow(E_F)$  is equal to zero [5]. The partial and total magnetic moments of ZrCoFeX (X=Si, As and Ge) are also computed as shown in Table 3. The total magnetic of ZrCoFeX (X=Si, As and Ge) is in line with the analytical proof of the Slater Paulin's rule ( $M_T = Z_T - 24$ )  $\geq 1$  for full or quaternary heuslers as our evaluated total magnetic moments are greater than one, which thus obey Slater Paulin's rule [7]. If  $M_T$  is greater than or equal to one it shows that the material is ferromagnetic but if it is equal to zero it is non-magnetic.

Table 3 Total and partial magnetic moments and Curie Temperature,  $T_c$  of ZrCoFeX (X=Si, As and Ge) (from *pdos.out* file) and the results of Bahnes in the Journal of Alloy and Compounds (2017) denoted by \*\*\*

Alloy	$M_{Zr}(\mu_B)$	$M_{Co}(\mu_B)$	$M_{Fe}(\mu_B)$	$M_X(\mu_B)$	$M_{Tot}(\mu_B)$	$T_c(K)$
ZrCoFeSi	0.6229	1.7486	0.7598	0.8902	4.0215	526
ZrCoFeAs	0.7831	1.6286	0.7693	0.9763	4.1573	859
ZrCoFeGe	0.8356	1.8748	0.9842	0.9765	4.6711	963
CoFeCrP ***	1.2220***	1.2630***	0.4060***	1.1111***	4.0000 ***	759 ***
CoFeCrAs ***	1.2300***	1.1553***	0.5050***	1.1120***	4.0000 ***	759 ***
CoFeCrSb ***	1.2000***	1.1830***	0.5060***	1.1110***	4.0000 ***	759 ***

### 3.3 Mechanical and Thermodynamic Properties

The calculated mechanical properties of ZrCoFeX (X=Si, As and Ge) such as elastic constants ( $C_{11}, C_{12}, C_{44}$ ), Shear modulus (G), Pugh's index ( $B/G$ ), Young's modulus, poisson's ratio ( $\nu$ ), Cauchy Pressure ( $C_{12} - C_{44}$ ) and Zener Anisotropy factor (A) are shown in Table 3. Our calculated elastic constants ( $C_{11}, C_{12}, C_{44}$ ) and Bulk modulus (B) are positive. This satisfies mechanical stability criteria given as  $C_{11} - C_{12} > 0$ ,  $C_{11} > 0$ ,  $C_{44} > 0$ ,  $(C_{11} + 2C_{12}) > 0$  and  $C_{12} < B < C_{11}$ , indicating that ZrCoFeSi, ZrCoFeAs and ZrCoFeGe have greater resistance against mechanical stress and deformations [10]. For ductility of material to be achieved Pugh's index, poisson's ratio and Cauchy Pressure must be greater than 1.75, 0.26 and positive respectively. From Table 3, our Pugh's index, poisson's ratio, Cauchy Pressure are 2.05, 1.82 and 3.25 respectively. This indicates that the quaternary heuslers are ductile. If these calculated values are less than that the given standard values, it means the materials are brittle.

For a material to be isotropic its Zener Anisotropic factor must be equal to unity (i.e 1), if it is greater than unity it is anisotropic. It must have the same alignment or orientation in all sides, and there is possibility of developing micro-cracks in future. However, our calculated value of Zener Anisotropy factor is greater than one ( $A > 1$ ), indicating that the material is anisotropic.

This is also shown in Table 3 [11]. However, for the sake of clarity equations of the mechanical properties are given here-under:

$$B_{VRH} = \frac{1}{2}(B_V + B_R), \quad B_{VRH} = \frac{1}{2} (G_V + G_R) \quad (6)$$

$$\text{Where } B_{V,R} = \frac{1}{3} (C_{11} + 2C_{12}), \quad G_R = \frac{5(C_{11}-C_{12})C_{44}}{4C_{44}-3(C_{11}-C_{12})}, \quad G_V = \frac{1}{5}(C_{11} - C_{12} + 3C_{44}) \quad (7)$$

The calculated elastic constants are listed in Table 3 with selected mechanical properties such as bulk, shear and Young's moduli, and Poisson's ratio. Isotropic Crystals are those which their atomic patterns have such a high degree of symmetry that their properties do not vary in different orientations (relative to their atomic patterns) [9]. Also, the Zener Anisotropy factor can be calculated by  $A = \frac{2C_{44}}{C_{11}-C_{12}}$  (8)

The value of A=1 gives purely isotropic system and the deviation from this value measures by percentage of Anisotropy, A<sub>G</sub>.

$$A_G = \frac{G_V - G_R}{G_V(G_V + G_R)} \quad (9)$$

If an alloy or compound has A greater than unity it shows that there is elastic anisotropy. Then, there will be possibility of developing more micro –cracks or structural defects during the growth process of the alloy or compound. Cauchy Pressure (CP) is also calculated in this work. It is shown by Petit that CP is given by  $CP = C_{12} - C_{44}$  (10)

Cauchy Pressure determines brittle or ductile nature of materials. CP value is a measure of metallic bonding or directional bonding with the angular character. If its value is positive, it indicates ductility and vice versa. Pugh's ratio B/G proposed by Pugh also measures ductility and brittleness ([8]. A material is said to have ductile behaviour if B/G ≈ 1.75. Any B/G value less than 1.75 shows brittleness of the material.

The Poisson's ratio V is another parameter for measuring ductility and brittleness.

$$V = \frac{(3B-2G)}{2(3B+G)} \quad (11)$$

If the value of  $V \approx 0.26$ , then the material is ductile and vice versa. The ratio of linear stress to strain is called Young's Modulus Y. Its higher value for a material means higher stiffness. With the increase in E, there is also increase in the covalent property of the material which has then impacted on the ductility of a material [4]. Young's modulus is defined in terms of bulk and shear moduli B and G as follows:

$$Y = \frac{9BG}{3G+B} \quad (12)$$

The higher value of E indicates stiffness of the material. Generally, the shear modulus G indicates the resistance to plastic deformation while Bulk modulus, B stands for resistance to fracture [9]. In fig. 4.0, stress-strain graphs of ZrCoFeX(X=Si, As and Ge) at different frequencies within their respective curie temperatures are plotted. Results show that ZrCoFeSi is susceptible to high stress up to 5.5Mpa with the strain effect of 0.5 at frequency 0.025s<sup>-1</sup>, This is followed by ZrCoFeAs of stress-strain effect of 1.5Mpa – 0.46 at frequency 0.12s<sup>-1</sup>. Stress-strain effect on ZrCoFeGe is low (1.3Mpa – 0.43) owing to its greater ferromagnetic strength, compared to the other two quaternaries. These indicate that effect of stress and strain on materials reduces their ductility etc.

The higher the stress-strain effect the less valued their mechanical stability, and hence the reduction in their ferromagnetism. ZrCoFeGe is more ferromagnetic than the other two heuslers as shown in Table 3.

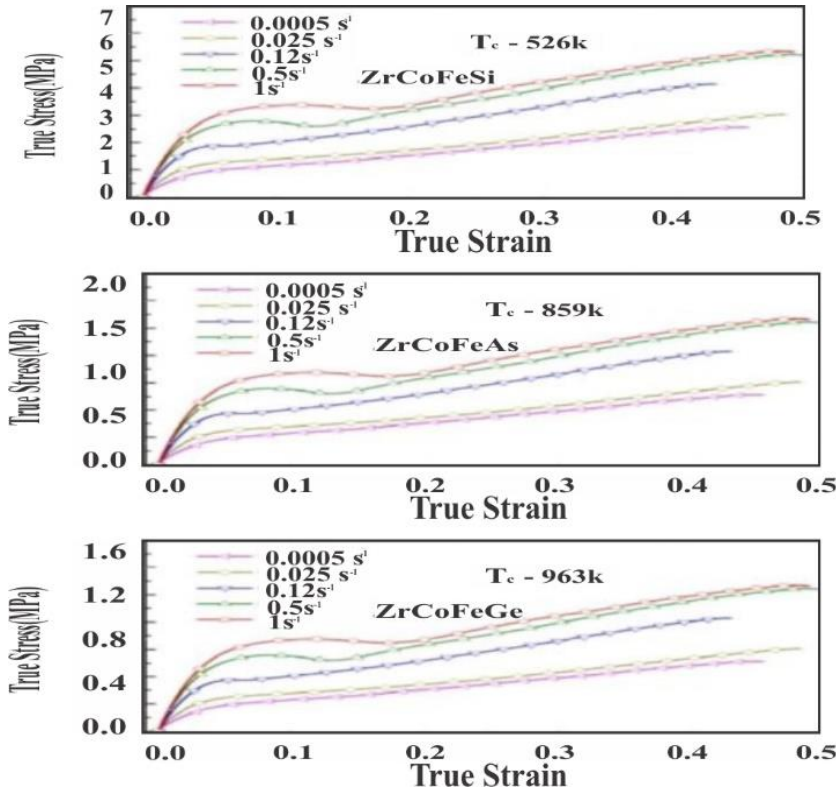


Fig.4. Stress-strain test of ZrCoFeX(X=Si, As and Ge) at different frequencies and curie temperatures

Table 1 Calculated Elastic constants ( $C_{ij}$ ) (Gpa), Bulk modulus ( $B$ )(Gpa),Shear modulus ( $G$ ) (Gpa),Young’s modulus( $Y$ ) (Gpa), Poisson’s ratio ( $\nu$ ), Anisotropy factor ( $A$ ), Pugh’s ratio ( $B/G$ ) and Cauchy’s Pressure ( $C_{12} - C_{44}$ ) of ZrCoFeSi ,ZrCoFeAs and ZrCoFeGe .and the results of CoFeCrZ(Z=P,As and Sb) \*\* by Bahnes (2017).

Heusler Alloy	$C_{11}$	$C_{12}$	$C_{44}$	$B$	$G$	$Y$	$\nu$	$A$	$B/G$	$C_{12} - C_{44}$
ZrCoFeSi	347	231	205	242	121	235	0.29	3.56	2.00	26
ZrCoFeAs	352	234	206	248	123	238	0.29	3.80	2.01	28
ZrCoFeGe	364	244	209	251	128	246	0.28	16.80	2.00	35
CoFeCrP**	265*	161*	128*	234*	89*	237*	0.33*	2.40*	2.63*	33**
	*	*	*	*	*	*	*	*	*	*
CoFeCrAs*	240*	190*	119*	209*	64*	174*	0.36*	4.82*	3.26*	71**
*	*	*	*	*	*	*	*	*	*	*
CoFeCrSb*	218*	268*	168*	185*	65*	174*	0.34*	4.74*	2.85*	100*
*	*	*	*	*	*	*	*	*	*	*

For thermodynamic properties of ZrCoFeX(X=Si, As and Ge), the heat capacity ( $C_V$ ) Versus temperature graphs are plotted in fig.4. This is in accordance with the thermodynamic equations below.

For classical thermodynamic process,

$$\langle n_s \rangle = \frac{1}{e^{\frac{\hbar\omega}{KT}} - 1} \quad (13)$$

The internal energy of the alloy is

$$E = \int_0^{\omega_D} \hbar\omega \langle n_s \rangle \sigma(\omega) d\omega \quad (14)$$

$$E = \int_0^{\omega_D} \hbar\omega \frac{1}{e^{\frac{\hbar\omega}{KT}} - 1} \cdot \frac{9N}{\omega_D^3} \omega^2 d\omega \quad (15)$$

$$\text{Putting } x = \frac{\hbar\omega_D}{KT}, \quad E = \frac{9N\hbar}{\omega_D^3} \left(\frac{KT}{\hbar}\right)^4 \int_0^{\frac{\hbar\omega_D}{KT}} \frac{x^3}{e^x - 1} dx \quad (16)$$

Let  $\theta_D = \frac{\hbar\omega_D}{K}$ . Then,  $\theta_D$  is the Debye characteristic Temperature

$$E = \frac{9N\hbar}{\omega_D^3} \left(\frac{KT}{\hbar}\right)^4 \int_0^{\frac{\theta_D}{T}} \frac{x^3}{e^x - 1} dx \quad (17)$$

Now, if  $T \gg \theta_D$ ,  $x_{max} = \frac{\hbar\omega_D}{KT} = \frac{\theta_D}{T}$  is small and, expanding the exponential and neglecting the higher powers;  $\frac{e^x}{e^x - 1} = x^2$

$$\text{Therefore, } E = \frac{9NKT^4}{\theta_D^3} \left[\frac{x^3}{3}\right]_{\theta_D/T}^{\theta_D/T} = \frac{9NKT^4}{\theta_D^3} \cdot \frac{\theta_D^3}{3T^3}, \quad E = 3NKT \quad (18)$$

This leads to the Dulong –Petit law

$$C_V = \left(\frac{\partial E}{\partial T}\right)_V = 3NK = 3R \quad (19)$$

Where  $R = KN$  is the molar gas constant.

Thus, for temperature greater than the Debye Temperature, the alloy behaves classically.

If on the other hand,  $T \ll \theta_D$ ,  $x \rightarrow \infty$ , then,

$$\int_0^{\infty} \frac{x^3 dx}{e^x - 1} = \int_0^{\infty} \frac{x^3 dx}{e^x(1 - e^{-x})} = \int_0^{\infty} x^3 e^{-x} (1 - e^{-x})^{-1} dx \quad (20)$$

$$= \int_0^{\infty} x^3 e^{-x} (1 - e^{-x} + e^{-2x} + e^{-3x} + \dots) dx \quad (21)$$

$$= \int_0^{\infty} x^3 \sum_{n=1}^{\infty} e^{-nx} dx \quad (22)$$

Using gamma function:  $\int_0^{\infty} x^3 \sum_{n=1}^{\infty} e^{-nx} dx = \sum_{n=1}^{\infty} \frac{3!}{n^4} = 3! \sum_{n=1}^{\infty} \frac{1}{n^4}$ , Using complex variables,  $\int_0^{\infty} \frac{x^3 dx}{e^x - 1} = \frac{6\pi^4}{90} = \frac{\pi^4}{15}$ ,

$$\text{Thus, } E = \frac{9NKT^4}{\theta_D^3}, \quad \frac{\pi^4}{15} = \frac{3\pi^4 NKT^4}{5\theta_D^3}, \quad \text{specific heat } C_V = \left(\frac{\partial E}{\partial T}\right)_V = \frac{3\pi^4 NK \partial T^4}{5\theta_D^3 \partial T} = \frac{3\pi^4 NK 4T^3}{5\theta_D^3} \quad (23)$$

$$C_V = \frac{12}{5} \pi^4 NK \quad (2)$$

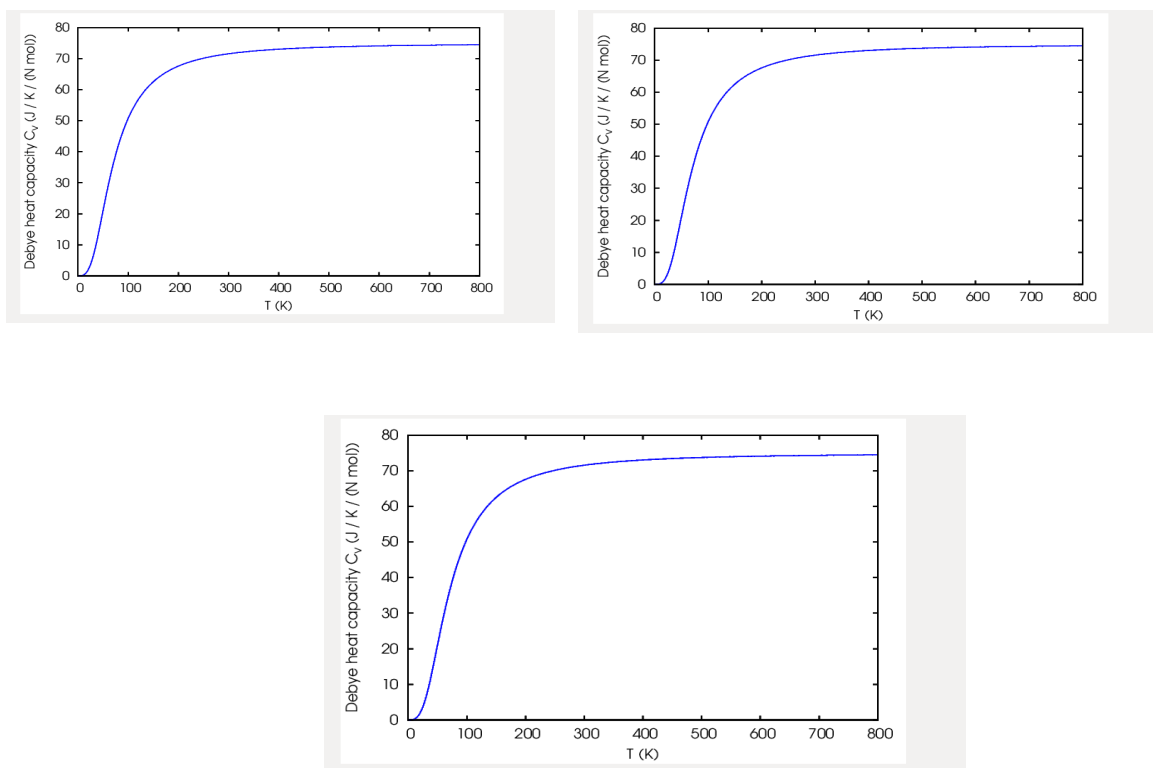


Fig.5 Heat Capacities Versus Temperatures of ZrCoFeX(X=Si, As and Ge)

The constant-volume heat capacity  $C_V$ , tends to the Dulong-Petit limit at high temperature (i.e it remains constant) but at sufficiently low temperature, the heat capacity of ZrCoFeSi, ZrCoFeAs and ZrCoFeGe is proportional to  $T^3$  [12]. This is verified analytically in eqs (5-15). It is observed that from 256K above, the constant-volume heat capacity for each heusler approaches asymptotic value of 78J/mol and obeys Dulong-Petit law which states that at high temperature heat capacity of material remains constant but at sufficiently low temperature (0k) the heat capacity of material is proportional to  $T^3$ , showing that it obeys  $T^3$  law at sufficiently low temperature and obeys Dulong-Petit law at high temperature.

This remarkable thermodynamic behaviour has good applications in the field of solid states physics where half-metallicity, ferromagnetism or 100% spin-polarization is great importance in spintronics, optoelectronics etc.

## CONCLUSION

First Principle calculations have been used to study the half-metallic behaviour, structural, mechanical, magnetic, electronic and thermodynamic properties of quaternary heuslers ZrCoFeX(X=Si, As and Ge). The results of the structural properties show that the heusler alloys are structurally stable and can be synthesized experimentally. All mechanical properties of the quaternary heuslers obey mechanical stability criteria as they show high ductility and greater resistance against deformations. The electronic band structures of ZrCoFeX(X=Si, As and Ge) give indirect band gaps which justifies their half-metallic character and 100% spin-polarization at the fermi energy levels. The total magnetic moments of the heusler alloys obey Slater-Paulin's rule, which indicates that the materials are ferromagnetic as ZrCoFeGe shows greater ductility and ferromagnetism. Thermodynamic heat capacities of ZrCoFeX(X=Si, As and Ge) show good thermal behaviour as it obeys  $T^3$  law at sufficiently low temperature and also obeys Dulong-Petit

law at high temperature. This portrays great potentials of the quaternary heuslers in the field of spintronic, optoelectronics etc. Our results are in good agreement with the results in literatures.

## REFERENCES

- [1] Akriche, A.; Bouafia, H.; Hiadsi, S.; Abidri, B.; Sahli, B.; Elchikh, M.; Djebour, B. First-principles study of mechanical, exchange interactions and the robustness in  $\text{Co}_2\text{MnSi}$  full Heusler compounds. *J. Magn. Magn. Mater.* 2017, 422, pg.13–19.
- [2] Alijani, V.; Ouardi, S.; Fecher, G.H.; Winterlik, J.; Naghavi, S.S.; Kozina, X.; Ueda, S. Electronic, structural, and magnetic properties of the half-metallic ferromagnetic quaternary Heusler compounds  $\text{CoFeMnZ}$  ( $Z = \text{Al, Ga, Si, Ge}$ ). *Phys. Rev. B* 2011, 84, pg.22-44.
- [3] Andrea M., Conor H., Myrta G. Yambo ab initio calculation tool for excited state calculations. 2008, 50, pg.1-20.
- [4] Atifi Sattar M., Muhammad Rashid, Raza Hashmi, Fayyat Hussain. study of half-metallicity *Journal of Chinese Physical Society and IOP.* 2016, Vol.25, No.10. pp10702-7
- [5] Babalola M.I, Iyozor B.E: A search for half-metallicity in half-Heusler alloys,  $\text{HfFeBi}$  and  $\text{TiFeBi}$  . *Journal of magnetism and magnetic materials.* 2019 ,165560, pp491-506.
- [6] Babiker, S.; Gao, G.; Yao, K. Half-metallicity and magnetism of Heusler alloys  $\text{CO}_2\text{HfZ}$  ( $Z = \text{Al, Ga, Ge, Sn}$ ). *J. Magn. Magn. Mater.* 2017, 441, pg.356–360.
- [7] Bahnes A., Boukortt A., Abbassa H., Almough D.E, Hyan A. Zaoul. Half-metallic ferromagnetic behaviour of a new quaternary Heusler compounds  $\text{CoFeCrZ}$  ( $Z = \text{P, As, and Sb}$ ). *Journal. of Alloys and Compounds.* 2017, 424, pg.22–77.
- [8] Bainsla, L.; Mallick, A.I.; Raja, M.M.; Nigam, A.K.; Varaprasad, B.C.S.; Takahashi, Y.K.; Hono, K. Spin gapless semiconducting behavior in equiatomic quaternary  $\text{CoFeMnSi}$  Heusler alloy. *Phys. Rev. B* 2015a, 91, pg.104-408.
- [9] Bainsla, L.; Mallick, A.I.; Coelho, A.A.; Nigam, A.K.; Varaprasad, B.C.S.; Takahashi, Y.K.; Hono, K. High spin polarization and spin splitting in equiatomic quaternary  $\text{CoFeCrAl}$  Heusler alloy. *J. Magn. Magn. Mater.* 2015b, 394, pg.82–86.
- [10] Bainsla, L.; Suresh, K.G., Artimeb B.V. Equiatomic quaternary Heusler alloys: A material perspective for spintronic applications. *Appl. Phys. Rev.* 2016, 031101 pg.32-45.
- [11] Blöch, P.E., Avengular B.N, Chenvzenco F.K. Projector augmented-wave method. *Phys. Rev. B* 2018, 50, pg.17-53.
- [12] Born, M., Huang K.L, Hoboken N.J, John W. Dynamical Theory of crystal Lattices. “Born-Oppenheimer Approach: Diabatization and Topological Matrix” Beyond Born-Oppeheimer : Electronic Nonadiabatic coupling Terms and conical Intersection . 2006, *Journal of phy. Rev.*, 2246, pg. 26-57.
- [13] Chibani, S.; Arbouche, O.; Zemouli, M.; Amara, K.; Benallou, Y.; Azzaz, Y.; Ameri, M. AbInitio Prediction of the Structural, Electronic, Elastic, and Thermoelectric Properties of Half-Heusler Ternary Compounds  $\text{TiIrX}$  ( $X = \text{As and Sb}$ ). *J. Electron. Journal of Mater. Sc.*, 2018, 47, pg.196–204.

- [14] De Groot, R.A.; Mueller, F.M.; Van Engen, P.G.; Buschow, K.H.J. New class of materials: Half-metallic ferromagnets. Phys. Rev. Lett. 1983, 50, pg.20-24.
- [15] Fazian M., Murtaza G., Sikandar A., Saleem A.K, Asif M., Elastic and Optoelectronic properties of novel Ag<sub>3</sub>AuSe<sub>2</sub> and Ag<sub>3</sub>AuTe<sub>2</sub> semiconductors. Journal of material science in semiconductor processing. 2016, 4537, pg.8–15.
- [16] Feng, Y.; Chen, X.; Zhou, T.; Yuan, H.; Chen, H. Structural stability, half-metallicity and magnetism of the CoFeMnSi/GaAs interface. Appl. Surf. Sci. 2015,346, pg.1–10.
- [17] Feng, Y.; Xu, X.; Cao, W.; Zhou, T. Investigation of cobalt and silicon co-doping in quaternary Heusler alloy NiFeMnSn. Comput. Mater. Sci. 2018, 147, pg. 251–257.

## APPENDIX: Supplementary analytical Details

### 1. Formation energy and cohesive energy of Quaternary Heusler ZrCoFeX (X=Si, As and Ge).

#### Formation energy

(a)  $E_f(\text{Zr}) = -6224.20768741\text{Ry}$  (from Zr.scf.out file) ,  $E_f(\text{Co}) = -6229.23199006\text{Ry}$  (from Co.scf.out file)

$E_f(\text{Fe}) = -6225.27851354\text{Ry}$  (from Fe.scf.out file ,  $E_f(\text{Si}) = -3625.27851354\text{Ry}$  (from Si.scf.out file)

$E_f(\text{As}) = -3625.27851354\text{Ry}$  (from Si.scf.out file),  $E_f(\text{Ge}) = -3625.27851354\text{Ry}$  (from Si.scf.out file)

$E_f(\text{ZrCoFeSi}) = -1542.89460937\text{Ry}$  (from ZrCoFeSi.scf.out file in band file of fm folder)

$E_f(\text{ZrCoFeAs}) = -1542.75705013\text{Ry}$  (from ZrCoFeAs.scf.out file in band file of fm folder )

$E_f(\text{ZrCoFeGe}) = -1542.89460937\text{Ry}$  (from ZrCoFeGe.scf.out file in band file of fm folder)

Therefore,  $E_f(\text{ZrCoFeSi}) = (E_f(\text{Total}) - E_f \frac{(\text{Zr})}{2} + E_f \frac{(\text{Co})}{2} + E_f(\text{Fe}) + E_f \frac{(\text{Si})}{4}$

$$E_f(\text{ZrCoFeSi}) = (-1742.89460937 - (\frac{-714.20768741}{2} + E_f \frac{(-614.20768741)}{2} + (-429.23667106) + (\frac{-3625.27851354}{4}))$$

$$E_f(\text{ZrCoFeSi}) = -1742.89460 - (-1542.655462) ,$$

$$E_f(\text{ZrCoFeSi}) = -1.6864\text{Ry}.$$

(b)  $E_f(\text{ZrCoFeAs}) = E_f(\text{Total}) - E_f \frac{(\text{Zr})}{2} + E_f \frac{(\text{Co})}{2} + E_f(\text{Fe}) + E_f \frac{(\text{As})}{4}$

$$E_f(\text{ZrCoFeAs}) = -1742.76705013 - (-1542.785462)$$

$$E_f(\text{ZrCoFeAs}) = -1.75635\text{Ry}$$

$$(c)E_f(ZrCoFeGe)= E_f(Total) - E_f \frac{(Zr)}{2} + E_f \frac{(Co)}{2} + E_f(Fe) + E_f \frac{(Ge)}{4}$$

$$E_f(ZrCoFeGe) = -1742.89460937 -(-1542.655462)$$

$$E_f(ZrCoFeSi) = -1.8439\text{Ry.}$$

### COHESIVE ENERGY

For ZrCoFeSi ,

$$E_{Coh}^{ZrCoFeSi} = E_{atom}^{(Zr)} + E_{atom}^{(Co)} + E_{atom}^{(Fe)} + E_{atom}^{(Si)} - E_{Total}^{(ZrCoFeSi)}$$

$$E_{Coh} = \left(\frac{(Zr)}{2} + E_f \frac{(Co)}{2} + E_f(Fe) + E_f \frac{(Si)}{4} - E_f(Total)\right)$$

$$E_{Coh} = \left(\frac{(-614.20768741)}{2} + (-329.23199006) + \left(\frac{(-3625.27851354)}{4}\right) - (-1542.89460937)\right)$$

$$E_{Coh} = 1.686405\text{Ry}$$

For ZrCoFeAs,

$$E_{Coh}^{ZrCoFeAs} = E_{atom}^{(Zr)} + E_{atom}^{(Co)} + E_{atom}^{(Fe)} + E_{atom}^{(As)} - E_{Total}^{(ZrCoFeAs)}$$

$$E_{Coh}^{ZrCoFeAs} = \left(\frac{(-614.20768741)}{2} + (-329.23199006) + \left(\frac{(-3625.27851354)}{4}\right) - (-1542.75705013)\right)$$

$$E_{Coh}^{ZrCoFeAs} = 1.7391\text{Ry}$$

For ZrCoFeGe,

$$E_{Coh}^{ZrCoFeGe} = E_{atom}^{(Zr)} + E_{atom}^{(Co)} + E_{atom}^{(Fe)} + E_{atom}^{(Ge)} - E_{Total}^{(ZrCoFeGe)}$$

$$E_{Coh}^{ZrCoFeAs} = \left(\frac{(-614.20768741)}{2} + (-329.23199006) + \left(\frac{(-3625.27851354)}{4}\right) - (-1542.89460937)\right)$$

$$E_{Coh}^{ZrCoFeAs} = 1.83995\text{Ry.}$$

### (2) MAGNETIC MAGNETIC MOMENTS OF ZrCoFeX(X=Si, As and Ge ).

*For ZrCoFeSi (From Pdos.out file of ZrCoFeSi folder)*

Polarization of Ni atom = 0.6229, Polarization of Co atom = 1.7486, Polarization of Fe atom = 0.7598

Polarization of Si atom = 0.8902. Total magnetic moment,  $M_{tot} = 0.6229 + 1.7486 + 0.7598 + 0.8903 = 4.0215\mu\text{B}$

*For ZrCoFeAs (From Pdos.out file of ZrCoFeAs folder)*

**Sunday and Sabo - Transactions of NAMP 24, (2026) 71-88**

Polarization of Ni atom = 0.7831, Polarization of Co atom = 1.6286, Polarization of Fe atom = 0.7693

Polarization of As atom = 0.9763. Total magnetic moment,  $M_{\text{tot}} = 0.7831 + 1.6286 + 0.7693 + 0.9763 = 4.1573 \mu\text{B}$

**For ZrCoFeGe (From Pdos.out file of ZrCoFeGe folder)**

Polarization of Zr atom = 0.8356, Polarization of Co atom = 1.8748, Polarization of Fe atom = 0.9842

Polarization of Ge atom = 0.9765. Total magnetic moment,  $M_{\text{tot}} = 0.8356 + 1.8748 + 0.9842 + 0.9765 = 4.6711 \mu\text{B}$ .

**(3) SPIN-POLARIZATION OF ZrCoFeX (X=Si, As and Ge).**

$$\begin{aligned} \text{Spin Polarization Percentage (P\%)} \text{ of ZrCoFeSi} &= \frac{P\uparrow(E_f) - P\downarrow(E_f)}{P\uparrow(E_f) + P\downarrow(E_f)} \times 100\% \\ &= \frac{0.206 - 0}{0.206 + 0} \times 100\% = 100\% \end{aligned}$$

$$\begin{aligned} \text{Spin Polarization Percentage (P\%)} \text{ of ZrCoFeAs} &= \frac{P\uparrow(E_f) - P\downarrow(E_f)}{P\uparrow(E_f) + P\downarrow(E_f)} \times 100\% \\ &= \frac{0.205 - 0}{0.205 + 0} \times 100\% = 100\% \end{aligned}$$

$$\begin{aligned} \text{Spin Polarization Percentage (P\%)} \text{ of ZrCoFeGe} &= \frac{P\uparrow(E_f) - P\downarrow(E_f)}{P\uparrow(E_f) + P\downarrow(E_f)} \times 100\% \\ &= \frac{0.203 - 0}{0.203 + 0} \times 100\% = 100\% \end{aligned}$$

**(4) THE CURIE TEMPERATURE,  $T_C$ , OF ZrCoFeX (X=Si, As and Ge).**

$T_C = \frac{\Delta E}{3K_B}$ , where  $\Delta E = E_{NM} - E_{FM}$  from alat.out file of Nm and FM folder of ZrCoFeX (X=Si, As and Ge).  $E_{NM}$  and  $E_{FM}$  are the total energies of ZrCoFeX (X=Si, As and Ge) from NM and FM

For ZrCoFeSi,  $E_{FM} = -1542.89\text{Ry}$ ,  $E_{NM} = -1542.88\text{Ry}$ ,

$$\Delta E = -1542.78 + 1546.96 = 0.01\text{Ry}, \quad 1\text{Ryberg} = 2.1798 \times 10^{-18}\text{J}$$

$$\Delta E = 10^{-2} \times 2.1798 \times 10^{-18}\text{J} = 2.1798 \times 10^{-20}\text{J}, \quad T_C = \frac{2.1798 \times 10^{-20}}{3 \times 1.38 \times 10^{-23}}\text{K}.$$

$$T_C = 526\text{K}.$$

For ZrCoFeAs,  $E_{FM} = -1542.89\text{Ry}$ ,  $E_{NM} = -1542.88\text{Ry}$ ,

$$\Delta E = -1542.88 + 1542.89 = 0.01\text{Ry}, \quad 1\text{Ryberg} = 2.1798 \times 10^{-18}\text{J}$$

$$\Delta E = 10^{-2} \times 2.1798 \times 10^{-18}\text{J} = 2.1798 \times 10^{-20}\text{J}, \quad T_C = \frac{2.1798 \times 10^{-20}}{3 \times 1.38 \times 10^{-23}}\text{K}.$$

$$T_C = 859K$$

For ZrCoFeGe,  $E_{FM} = -1542.76Ry$ ,  $E_{NM} = -1542.71Ry$

$$\Delta E = -1542.71 + 1542.728 = 0.01829Ry,$$

$$\Delta E = 1.829 \times 2.1798 \times 10^{-20} J ,$$

$$T_C = \frac{3.987 \times 10^{-20}}{3 \times 1.38 \times 10^{-23}} K , T_C = 963K$$

**(5) Half-Metallic Gap of ZrCoFeX (X=Si, As and Ge).**

$HM_{Gap} = \min(|E_f - E_{VBM}|, |E_f - E_{CBM}|)$ , where  $E_f$ ,  $E_{VBM}$ ,  $E_{CBM}$  are the Fermi energy, valence band maximum ( $E_{VBM}$ ) Energy and Conduction band minimum (CBM) Energy respectively.

For ZrCoFeSi,  $HM_{Gap} = \min(|0 - (-0.205)|, |0 - 0.3|) = \min(0.205), (0.3)$

Thus, the minimum value is 0.205eV . ∴ ,  $HM_{Gap}$  of ZrCoFeSi =0.205eV

For ZrCoFeAs,  $HM_{Gap} = \min(|0 - (-0.206)|, |0 - 0.4|) = \min(0.206), (0.4)$

Thus, the minimum value is 0.206eV . ∴ ,  $HM_{Gap}$  of ZrCoFeAs =0.206eV

For ZrCoFeGe,  $HM_{Gap} = \min(|0 - (-0.203)|, |0 - 0.4|) = \min(0.203), (0.4)$

Thus, the minimum value is 0.203eV . ∴  $HM_{Gap}$  of ZrCoFeGe =0.203eV

**(6) MECHANICAL PROPERTIES OF ZrCoFeX(X=Si, As and Ge)**

**For ZrCoFeSi:**  $C_{11}=347Gpa$ ,  $C_{12}=231Gpa$ ,  $C_{44}=205Gpa$  (From output file of Thermo\_pw code)

$$B = B_{VRH} = \frac{1}{2}(B_V + B_R) = \frac{1}{2}(242.99 + 241.91) = 242Gpa$$

$$G = G_{VRH} = \frac{1}{2}(G_V + G_R) = \frac{1}{2}(121.02 + 121.22) = 121Gpa$$

$$\text{Young's modulus, } Y = E_{VRH} = \frac{1}{2}(Y_V + Y_R) = \frac{1}{2}(235.38 + 235.39) = 235Gpa$$

$$\text{Poisson's ratio, } \nu = \frac{3B-2G}{2(3B+G)} = \frac{3(242)-(2 \times 121)}{2(3 \times 242+121)} = 0.29$$

Cauchy Pressure,  $CP = C_{12} - C_{44} = 231 - 205 = 26Gpa$ .

$$\text{Anisotropic factor, } A = \frac{2C_{44}}{C_{11}-C_{12}} = \frac{2 \times 205}{347-231} = 3.53, \text{ Pugh's ratio, } B/G = \frac{242}{121} = 2.00$$

**For ZrCoFeAs:**  $C_{11}=352Gpa$ ,  $C_{12}=324Gpa$ ,  $C_{44}= 206Gpa$  (From output file of Thermo\_pw ccode)

$$B_{VRH} = \frac{1}{2}(B_V + B_R) = \frac{1}{2}(248.09 + 248.11) = 248Gpa$$

$$G = G_{VRH} = \frac{1}{2}(G_V + G_R) = \frac{1}{2}(123.11 + 123.22) = 123.01Gpa$$

**Sunday and Sabo - Transactions of NAMP 24, (2026) 71-88**

$$\text{Young's modulus, } Y = E_{VRH} = \frac{1}{2}(Y_V + Y_R) = \frac{1}{2}(238.11 + 238.39) = 238\text{Gpa}$$

$$\text{Poisson's ratio, } \nu = \frac{3B-2G}{2(3B+G)} = \frac{3(248)-(2 \times 123)}{2(3 \times 248+123)} = 0.29$$

$$\text{Cauchy Pressure, } CP = C_{12} - C_{44} = 244 - 206 = 38\text{Gpa.}$$

$$\text{Anisotropic factor, } A = \frac{2C_{44}}{C_{11}-C_{12}} = \frac{2 \times 206}{352-244} = 3.8, \text{ Pugh's ratio, } B/G = \frac{248}{123} = 2.01$$

**For ZrCoFeGe:**  $C_{11}=364\text{Gpa}$ ,  $C_{12}=324\text{Gpa}$ ,  $C_{44}=209\text{Gpa}$  (From output file of Thermo\_pw code)

$$B = B_{VRH} = \frac{1}{2}(B_V + B_R) = \frac{1}{2}(251.11 + 251.21) = 251\text{Gpa}$$

$$G = G_{VRH} = \frac{1}{2}(G_V + G_R) = \frac{1}{2}(128.12 + 128.22) = 128\text{Gpa}$$

$$\text{Young's modulus, } Y = E_{VRH} = \frac{1}{2}(Y_V + Y_R) = \frac{1}{2}(246.11 + 246.12) = 246\text{Gpa}$$

$$\text{Poisson's ratio, } \nu = \frac{3B-2G}{2(3B+G)} = \frac{3(251)-(2 \times 128)}{2(3 \times 251+128)} = 0.28$$

$$\text{Cauchy Pressure, } CP = C_{12} - C_{44} = 324 - 209 = 115\text{Gpa.}$$

$$\text{Anisotropic factor, } A = \frac{2C_{44}}{C_{11}-C_{12}} = \frac{2 \times 324}{364-324} = 16.8, \text{ Pugh's ratio, } B/G = \frac{251}{128} = 2.00$$

**(7) Electronic Configuration of Zirconium, Cobalt, Iron, Silicon, Arsenic and Germanium**

$$\begin{aligned} \text{Zr}=40 &= 1S^2 2S^2 2P^6 3S^2 3P^6 4S^2 3d^{10} 4P^6 5S^2 4d^2, & \text{Co} &= 27 = \\ 1S^2 2S^2 2P^6 3S^2 3P^6 4S^2 3d^7, & \text{Fe} &= 26 = 1S^2 2S^2 2P^6 3S^2 3P^6 4S^2 3d^6 & \text{Si} &= 14 = \\ 1S^2 2S^2 2P^6 3S^2 3P^2, & \text{As} &= 33 = 1S^2 2S^2 2P^6 3S^2 3P^6 3d^{10} 4S^2 4p^3, \end{aligned}$$

**Valence Electrons ( $Z_T$ )**

$$\text{Zr} = 5S^2 4d^2, \text{ Co} = 3d^7 4S^2, \text{ Fe} = 3d^6 4S^2, \text{ Si} = 3S^2 3P^2, \text{ As} = 3d^{10} 4S^2 4p^3, \text{ Ge} = 3d^{10} 4S^2 4p^2$$

$$\text{For ZrCoFeSi, Total valence electrons } (Z_T) = 10+9+8+4 = 31$$

$$\text{By Slater Paulin's rule, } M_T = |Z_T - 24| \geq 1 \text{ for Full or Quaternary Heuslers, } M_T = |31 - 24| = 7$$

$$\text{For ZrCoFeAs, Total valence electrons } (Z_T) = 10+9+8+15=42, M_T = |42 - 24| = 18$$

$$\text{For ZrCoFeGe, Total valence electrons } (Z_T) = 10+9+8+14=41, M_T = |41 - 24| = 17$$

Therefore, ZrCoFeX(X=Si, As and Ge) is ferromagnetic